Coherent deeply virtual Compton scattering off ^{4}He

Sara Fucini,[1] Sergio Scopetta,[1] and Michele Viviani[2]
[1]*Dipartimento di Fisica e Geologia, Università degli Sudi di Perugia, and INFN, Sezione di Perugia, via A. Pascoli, I-06123 Perugia, Italy*
[2]*INFN-Pisa, 56127 Pisa, Italy*

(Received 18 May 2018; published 12 July 2018)

Coherent deeply virtual Compton scattering off the ^{4}He nucleus is studied in impulse approximation. A convolution formula for the nuclear generalized parton distribution (GPD) is derived in terms of the ^{4}He one-body nondiagonal spectral function and of the GPD of the struck nucleon. A model of the nuclear nondiagonal spectral function, based on the momentum distribution corresponding to the Argonne 18 nucleon-nucleon interaction, is used in the actual calculation. Typical impulse approximation results are reproduced, in proper limits, for the nuclear form factor and for nuclear parton distributions. The nuclear generalized parton distribution and the Compton form factor are evaluated using, as a nucleonic ingredient, a well-known generalized parton distribution model. An overall very good agreement is found with the data recently published by the EG6 experiment at the Jefferson Laboratory (JLab). More refined nuclear calculations are addressed and will be necessary for the expected improved accuracy of the next generation of experiments at JLab with the 12-GeV electron beam and high luminosity.

DOI: 10.1103/PhysRevC.98.015203

I. INTRODUCTION

Nuclear generalized parton distributions (GPDs), measured in hard-exclusive electroproduction processes in nuclei, can provide a wealth of novel information (for a recent report, see, i.e., Ref. [1]), such as a signature of the presence of non-nucleonic degrees of freedom [2] or a nuclear tomography, i.e., the distribution of partons with a given longitudinal momentum on the nuclear transverse plane. Nuclear GPDs can be therefore very important for a fully quantitative explanation of the so-called European Muon Collaboration (EMC) effect [3], i.e., the nuclear modifications of the parton structure of bound nucleons (see Ref. [4] for a recent report).

Several processes can be described in terms of GPDs. Among them, the one of interest here is coherent deeply virtual Compton scattering (DVCS), i.e., deep exclusive photon electroproduction off a nuclear target A, the hard fully exclusive reaction $A(e,e'\gamma)A$, which could give access to the quark tomography of the nucleus as a whole. The experimental study of this process requires the very difficult coincidence detection of fast photons and electrons together with slow intact recoiling nuclei. For this reason, in the first measurement of nuclear DVCS from the HERMES Collaboration [5], a clear separation was not achieved between the coherent process and the so-called incoherent one, i.e., the process $A(e,e'\gamma N)X$, which allows the tomography of the bound nucleon. The latter, compared with that of the free nucleon, could provide a pictorial view of the realization of the EMC effect.

Much theoretical work has been performed to study nuclear GPDs (see Ref. [1] for a review of results). We remind that, measuring GPDs through DVCS, it has been suggested to study the distribution of nuclear forces in nuclei [6–8] and the modifications of the bound nucleon structure [9–17]. The general formalism of DVCS on nuclear targets of any spin has been developed initially in Ref. [18].

In these studies, a special role is played by few nucleon systems, such as ^{2}H, ^{3}He, and ^{4}He. As a matter of fact, although challenging, for these targets a realistic evaluation of conventional nuclear effects is possible. This would allow to distinguish these effects from exotic ones, which could be responsible of the observed EMC behavior. Without realistic benchmark calculations, the interpretation of the collected data will be hardly conclusive. In this sense, the use of heavier targets due to the difficulty of the corresponding realistic many-body calculations, is less promising. The ^{2}H nucleus is very interesting for the extraction of the neutron information and for its rich spin structure [2,19,20]. In between ^{2}H and ^{4}He, ^{3}He could allow for studying the A dependence of nuclear effects, and it could give easy access to neutron polarization properties due to its specific spin structure. Besides, being not isoscalar, flavor dependence of nuclear effects could be studied, in particular, if parallel measurements on ^{3}H targets were possible. A complete impulse approximation (IA) analysis, using the Argonne 18 (Av18) nucleon-nucleon potential [21], is available, and nuclear effects on GPDs are found to be sensitive to details of the used nucleon-nucleon interaction [22–26]. Measurements for ^{2}H and ^{3}He have been addressed, planned in some cases, but they have not been performed yet.

From the theoretical side, ^{4}He is a very important system: Although really challenging, realistic calculations are possible; besides, ^{4}He is deeply bound, and therefore it represents the prototype of a typical finite nucleus; in addition to that, it is spinless so that experimentally targets are easy to be implemented and data are easy to be analyzed. Measurements were addressed, and theoretical predictions were proposed in Refs. [27–29]. The first data for coherent DVCS off ^{4}He have been recently published [30] and for the incoherent channel have been already collected at JLab by the EG6 experiment of the CLAS Collaboration with the 6-GeV electron beam. For the first time a successful separation of coherent and incoherent

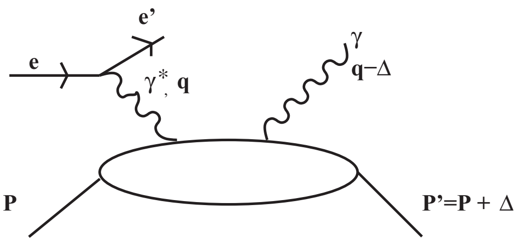

FIG. 1. The generic coherent DVCS process off a target A.

contributions has been achieved. A new impressive program is on the way at JLab12, carried on by the ALERT Collaboration [31,32]. In Ref. [30], the importance of new calculations has been addressed for a completely successful description of the collected data, not possible with the models proposed a long time ago, corresponding in some cases to different kinematical regions. New refined calculations are certainly important, above all, for the next generation of accurate measurements.

Here, a conventional IA analysis of the ^{4}He GPD and the nuclear Compton form factor (ff) is presented. The actual calculation is performed with basic nuclear and nucleonic ingredients, and the results are compared with the recently published data [30].

The paper is structured as follows. In the second section, the formalism is introduced. In the third one, nuclear and nucleonic ingredients of the actual calculation are presented. Then, numerical results are shown and discussed in the fourth section. Eventually, conclusions and perspectives are given.

II. FORMALISM

The most general coherent DVCS process $A(e,e'\gamma)A$ is shown in Fig. 1. If the momentum transferred by the electrons Q^2 is much higher than $-t = -\Delta^2 = -(P - P')^2$, the momentum transferred to the hadronic system with initial (final) four-momentum $P(P')$, the hard vertex of the "handbag" diagram depicted in Fig. 2 can be studied perturbatively, whereas the soft part, given by the blob in the figure, is parametrized in terms of GPDs, thanks to the factorization property demonstrated in Ref. [33].

The formalism for DVCS off a scalar target, exploiting only one chiral even GPD at a leading twist, has been developed in Ref. [29]. In the following, a workable expression for $H_q^{^4\mathrm{He}}$, the GPD of the quark of flavor q in the ^{4}He nucleus, will be derived within the IA description of the handbag approximation, depicted in Fig. 3.

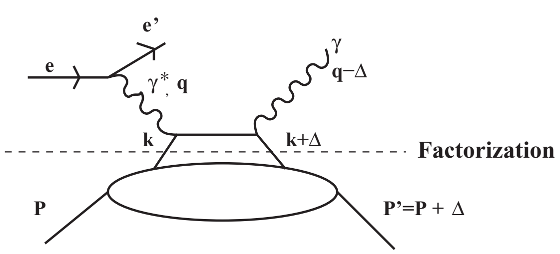

FIG. 2. The handbag approximation to the process shown in Fig. 1.

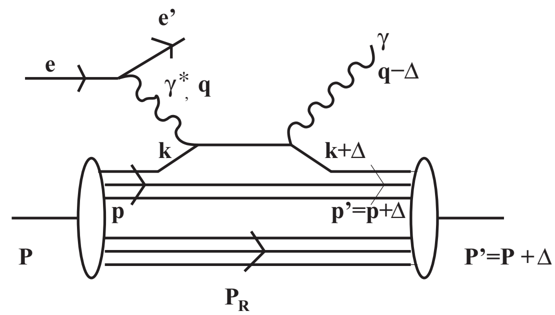

FIG. 3. The impulse approximation description of the handbag process shown in Fig. 2.

From the expression of the leading twist light-cone correlator, one can define H_q^A for a generic scalar target [34],

$$H_q^A(x,\xi,\Delta^2) = (2P+\Delta)^+ \int \frac{dr^-}{4\pi} e^{ix\bar{P}^+ r^-} \times \langle P'|\bar{\psi}_q\left(-\frac{r^-}{2}\right)\gamma^+\psi_q\left(\frac{r^-}{2}\right)|P\rangle\Big|_{r^+=0,\vec{r}_\perp=0}. \quad (1)$$

In the above equation, the dependence of H_q^A on three scalars is explicitly shown. Besides Δ^2, GPDs depend on the skewness $\xi = \frac{P^+ - P'^+}{P^+ + P'^+} = -\frac{\Delta^+}{2\bar{P}^+}$, i.e., the difference in the plus momentum faction between the initial and the final states, completely fixed by the external lepton kinematics, and on x, the average plus momentum fraction of the struck parton with respect to the total momentum, not experimentally accessible.

The additional dependence of GPDs on the hard momentum scale Q^2 is not explicitly shown for an easy presentation. Here and in the rest of the paper, the light-cone coordinates corresponding to a generic four-vector $v = (v_0,\vec{v})$ are defined as $v^\pm = \frac{v^0 \pm v^3}{\sqrt{2}}$.

We recall that, in the case of zero-momentum transfer, i.e., in the forward limit ($P' = P$, i.e., $\Delta^2 = 0$, $\xi = 0$), $H_q^{^4\mathrm{He}}$ reduces to ^{4}He parton distributions (PDFs) accessed through deep inelastic-scattering (DIS) experiments,

$$H_q^{^4\mathrm{He}}(x,0,0) = q^{^4\mathrm{He}}(x), \quad (2)$$

whereas its first moment yields the electromagnetic form factor of ^{4}He,

$$\sum_q e_q \int_{-1}^{1} dx\, H_q^{^4\mathrm{He}}(x,\xi,\Delta^2) = F_C^{^4\mathrm{He}}(\Delta^2), \quad (3)$$

where e_q represents the charge of the quark of flavor q.

Besides, in the quark sector, one can define the plus momentum of the struck parton before and after the interaction,

$$k^+ = (x+\xi)\bar{P}^+, \quad (4)$$

$$k'^+ = (k+\Delta)^+ = (x-\xi)\bar{P}^+, \quad (5)$$

respectively. It is therefore clearly seen that x represents the average plus momentum fraction of the struck parton with respect to the total nucleus momentum.

Now, the IA to the handbag approximation, shown in Fig. 3, will be described. The interacting parton, with momentum k, belonging to a given nucleon with momentum p in the nucleus, interacts with the probe, and it is afterwords reabsorbed with four-momentum $k + \Delta$ by the same nucleon without further rescattering with the recoiling three-body system. One should note that, in this scheme, only nucleonic degrees of freedom occur explicitly in the nuclear description. In IA it is useful to rewrite the parton momenta also with respect to those of the inner nucleon N as follows:

$$\xi' = -\frac{\Delta^+}{2p_N^+}; \tag{6}$$

$$x' = \frac{\xi'}{\xi}x. \tag{7}$$

The IA framework in the instant form of dynamics described in Ref. [22] for ^{3}He is here extended to ^{4}He. The main steps are summarized here below. Initially, light-cone quantized states and operators are used. The tensor product of two complete sets of states can be inserted into the left- and the right-hand sides of the quark operator in Eq. (1); the first set corresponds to the nucleon N, supposed free, interacting with the virtual photon, whereas the second set describes the recoiling system, which consists of three fully interacting particles. Using the fact that the quark operator in Eq. (1) is a one-body operator, one can consider its action on the nucleonic degrees of freedom only. Separating the global motion from the intrinsic one, possible since at the end nonrelativistic wave functions are used, a convolution formula can be obtained

$$\begin{aligned}
&H_q^{^4\text{He}}(x,\xi,\Delta^2)\\
&= (2P+\Delta)^+\left[\int \frac{dr^-}{4\pi}e^{ix\bar{P}^+r^-}\right]\int dE\,\rho(E)\\
&\quad\times\sum_{p_N,\sigma,\alpha}\langle P+\Delta|-p_N,E\{\alpha\};p_N+\Delta,\sigma\rangle\\
&\quad\times\langle p_N,\sigma;p_N,E,\{\alpha\}|P\rangle\\
&\quad\times\left[\langle p_N+\Delta,\sigma|\bar{\psi}_q\left(-\frac{r^-}{2}\right)\gamma^+\psi_q\left(\frac{r^-}{2}\right)|p_N,\sigma\rangle\right],
\end{aligned} \tag{8}$$

where the terms in the square brackets can be rearranged in terms of the generic light-cone correlator for the nucleon N considered for states with the same polarization σ, that reads [34]

$$F_{++}^N = \sqrt{1-\xi^2}\left[H_q^N - \frac{\xi^2}{1-\xi^2}E_q^N\right]. \tag{9}$$

In the above equation, in the kinematical region of the coherent channel of interest here, the dominant term is given by the GPD H_q. Thus, in the following, we will consider only this contribution. Using Eq. (9) in Eq. (8) and properly considering the partonic variables (6) and (7), one arrives at a convolution formula,

$$H_q^{^4\text{He}}(x,\xi,\Delta^2) = \sum_N \int_{|x|}^1 \frac{dz}{z} h_N^{^4\text{He}}(z,\Delta^2,\xi) H_q^N\left(\frac{x}{z},\frac{\xi}{z},\Delta^2\right), \tag{10}$$

between the GPD H_q^N of the quark of flavor q in the bound nucleon N and the off-diagonal light-cone momentum distribution of N in ^{4}He, which reads

$$\begin{aligned}
h_N^{^4\text{He}}(z,\Delta^2,\xi) &= \int dE \int d\vec{p}\, P_N^{^4\text{He}}(\vec{p},\vec{p}+\vec{\Delta},E)\delta\left(z - \frac{\bar{p}^+}{\bar{P}^+}\right)\\
&= \frac{M_A}{M}\int dE\int d\vec{p}\,\frac{\tilde{M}}{p}\,P_N^{^4\text{He}}(\vec{p},\vec{p}+\vec{\Delta},E)\\
&\quad\times\delta\left(\tilde{z}\frac{\tilde{M}}{p} - \frac{p^0}{p} - \cos\theta\right)\\
&= \frac{M_A}{M}\int dE\int_0^{2\pi}d\phi\\
&\quad\times\int_{p_{\min}}^{\infty}dp\,p\,\tilde{M}P_N^{^4\text{He}}(\vec{p},\vec{p}+\vec{\Delta},E).
\end{aligned} \tag{11}$$

In the last step of the above equation, we defined $M(M_A)$ as the nucleon (nuclear) mass, $\xi_A = \frac{M_A}{M}\xi$, $\tilde{z} = \frac{M_A}{M}z + \xi_A$, and $\tilde{M} = \frac{M}{M_A}(M_A + \frac{\Delta^+}{\sqrt{2}})$. The explicit form for the lower limit of integration in $p = |\vec{p}|$ is given by

$$p_{\min}(z,\xi_A,E) = \frac{1}{2}\left|\frac{M_{A-1}^{*2} - M_A^2\left(1-\frac{\tilde{M}}{M_A}\tilde{z}\right)^2}{M_A\left(1-\frac{\tilde{M}}{M_A}\tilde{z}\right)}\right|, \tag{12}$$

result obtained imposing the natural support for the function $\cos\theta$ in the argument of the δ function in Eq. (11) with M_{A-1}^{*2} as the squared mass of the final $(A-1)$-body excited state.

The off-diagonal light-cone momentum distribution of the nucleon N in ^{4}He is defined through its nondiagonal spectral function,

$$\begin{aligned}
&P_N^{^4\text{He}}(\vec{p},\vec{p}+\vec{\Delta},E)\\
&\quad= \rho(E)\sum_{\{\alpha\}\sigma_N}\langle P+\Delta|-p\,E\,\alpha,p+\Delta\,\sigma_N\rangle\\
&\qquad\times\langle p\,\sigma_N,-p\,E\,\alpha|P\rangle
\end{aligned} \tag{13}$$

$$\quad= n_0(\vec{p},\vec{p}+\vec{\Delta})\delta(E) + P_1(\vec{p},\vec{p}+\vec{\Delta},E), \tag{14}$$

with $\rho(E)$ being the energy density for the final states. The overlaps appearing in this formula include wave functions of the recoiling three-body system, which can be a bound system, a two-body, or a three-body scattering state with any possible relative energy between the constituents. We reiterate that any interaction of the debris originating by the struck nucleon with the remnant $(A-1)$ nuclear system is instead disregarded as usual in the IA scheme.

The forward limit of the expression Eq. (14) leads to the one-body diagonal spectral function of ^{4}He, $P_N^{^4\text{He}}(\vec{p},E)$ so that Eq. (11) reduces to

$$\begin{aligned}
h_N^{^4\text{He}}(z,0,0) &= f_N^{^4\text{He}}(z)\\
&= \int dE\int d\vec{p}\,P_N^{^4\text{He}}(\vec{p},E)\delta\left(z - \frac{\sqrt{2}p^+}{M}\right).
\end{aligned} \tag{15}$$

Using this result, Eq. (10) reproduces in the forward limit the correct IA result for the nuclear PDF (see, e.g., Ref. [35]), in agreement with Eq. (2).

Besides, the x integral of Eq. (10) yields formally the IA, a one-body approximation to the nuclear form factor so that the constraint Eq. (3) is also formally fulfilled.

A few caveats have to be addressed:

(i) In the present instant form calculation the number of particle sum rules and the momentum sum rules cannot be fulfilled at the same time. In particular, the momentum sum rule is here violated by a few percent. To overcome this drawback a Poincarè covariant light-front (LF) approach could be used. Relevant steps towards this goal have been performed for a three-body nuclear target [36].

(ii) The present scheme is not covariant, and, as a consequence, the GPDs, although scalar, turn out to be frame dependent. For GPDs' calculation as well as for form factors at high-momentum transfer the use of LF dynamics would be the proper framework. Nevertheless, in the experiment discussed in the present paper, the momentum transfer is rather low, and we found that in the observables we are going to show the results in the laboratory frame or in the Breit frame differ at most by a few parts in 1000. Therefore, at the moment, this problem is not a numerically relevant one. The results presented later on have been obtained in the laboratory frame.

Concluding this section, one should note that, in the present IA approach, the momentum scale Q^2 of the nuclear GPD is entirely given by that of the nucleon GPD and, for the sake of a readable presentation, it is not explicitly written in the following.

III. SETUP OF THE CALCULATION

It is clear from the previous section that, in order to actually evaluate the ^{4}He GPD and then the cross section for coherent DVCS off ^{4}He, we need an input for the nuclear nondiagonal spectral function and for the nucleonic GPD.

Concerning the nuclear part, only old attempts exist for obtaining a spectral function of ^{4}He [37,38]. A realistic description of the two- and, above all, three-body scattering states in the recoiling system is a really complicated few-body problem. Moreover, one would need here a nondiagonal spectral function, a quantity rather more complicated than the diagonal one.

We have planned a full realistic calculation of the ^{4}He spectral function; however, in this paper, use of the following model has been performed:

$$\begin{aligned}
&P_N^{^4\mathrm{He}}(\vec{p},\vec{p}+\vec{\Delta},E)\\
&= n_0(\vec{p},\vec{p}+\vec{\Delta})\delta(E^*) + P_1(\vec{p},\vec{p}+\vec{\Delta},E^*)\\
&= n_0(|\vec{p}|,|\vec{p}+\vec{\Delta}|,\cos\theta_{\vec{p},\vec{p}+\vec{\Delta}})\delta(E^*)\\
&\quad + P_1(|\vec{p}|,|\vec{p}+\vec{\Delta}|,\cos\theta_{\vec{p},\vec{p}+\vec{\Delta}},E^*)\\
&\simeq a_0(|\vec{p}|)a_0(|\vec{p}+\vec{\Delta}|)\delta(E^*) + n_1(|\vec{p}|,|\vec{p}+\vec{\Delta}|)\delta(E^*-\bar{E}),
\end{aligned} \tag{16}$$

with the removal energy $E = |E_A| - |E_{A-1}| + E^*$ defined in terms of the ground-state binding energies of ^{4}He and of the recoiling three-nucleon system E_A and E_{A-1}, respectively, and in terms of the excitation energy of the recoiling system E^*. Besides, one has $n_1(|\vec{p}|) = n(|\vec{p}|) - n_0(|\vec{p}|)$ and

$$n_0(|\vec{p}|) = |a(|\vec{p}|)|^2, \tag{17}$$

with $a(|\vec{p}|)$ as the overlap of the wave functions of the four- and three-body bound systems,

$$a(|\vec{p}|) = \langle \Phi_3(1,2,3)\chi_4\eta_4 | j_0(|\vec{p}|R_{1\text{-}4})\Phi_4(1,2,3,4)\rangle. \tag{18}$$

In our calculation $n_0(k)$, the momentum distribution with the recoiling system in the ground state and the total momentum distribution $n(k)$ have been evaluated using variational wave functions for the four-body [41] and three-body [42] systems obtained through the hyperspherical harmonics method [43] within the Av18 NN interaction [21], including UIX three-body forces [44].

The spirit of the approximation Eq. (16) is the following. In the first line of the equation, the rotational invariance of the problem has been exploited, showing a dependence on the absolute values of the initial and final momenta of the struck nucleon and on the angle between these two momenta. In the second line, the so-called closure approximation to the spectral function is used in the excited sector described by the spectral function P_1, i.e., an average value of the removal energy is chosen so that the nondiagonal spectral function reduces to a nondiagonal momentum distribution. The average value $\bar{E}$ of the excitation energy E^* of the recoiling system is evaluated through the model diagonal spectral function, based on the same Av18 + UIX interaction, proposed in Refs. [45,46], representing a realistic update of the one presented in Ref. [47]. In the last step, also the angular dependence is disregarded so that the nondiagonal momentum distributions can be modeled on the basis of the known diagonal ones.

For the nucleonic part, the well-known GPD model elaborated by Goloskokov and Kroll (GK) [48,49] has been used. We recall here, for the reader's convenience, its main features. The explicit form of the GPDs is obtained fitting high-energy deeply virtual meson production data. This guarantees the access to the low-x region. The structure of the (x,ξ) dependence is built through the double-distributions representation [50] so that the polynomiality property is automatically satisfied, whereas the t dependence is parametrized using a Regge-inspired profile function. The model is valid in principle at Q^2 values larger than those of interest here, in particular, at $Q^2 \geqslant 4$ GeV^2.

IV. NUMERICAL RESULTS

With the ingredients presented in the previous section on hand, a numerical evaluation of the nuclear GPD Eq. (10) is possible, and a comparison with the related experimental observables, recently accessed by the EG6 experiment at JLab, can be performed. Before that, let us consider two useful numerical tests of the formalism.

First of all, one should recover the IA result for the electromagnetic ff (for example, the one-body result in Ref. [39]), by

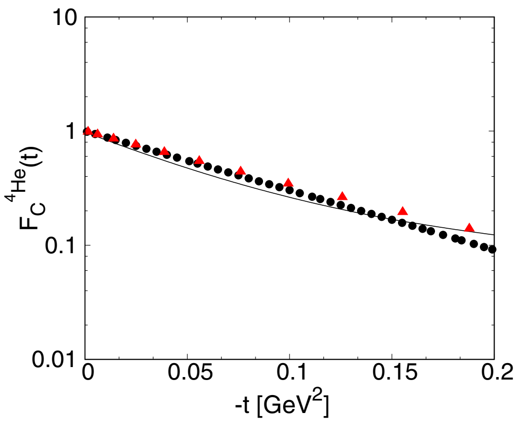

FIG. 4. The ^{4}He form factor obtained as the integral of the ^{4}He GPDs calculated in the present approach Eq. (10) (full), compared with data at low t (dots) [40], the ones relevant for the discussion presented here. The red triangles represent the one-body part of the Av18 + UIX (where UIX represents the Urbana-IX) calculation of the form factor shown in Ref. [39] (see the text).

x integration of the obtained GPD using Eq. (2),

$$\begin{aligned}
&\frac{1}{2}\sum_q e_q \int_{-1}^{1} dx\, H_q^{^4\mathrm{He}}(x,\xi,\Delta^2)\\
&= \frac{1}{2}\sum_{N,q} e_q \int_{-1}^{1} dx \int_{|x|}^{1} \frac{dz}{z} h_N^{^4\mathrm{He}}(z,\xi,\Delta^2) H_q^N\left(\frac{x}{z},\frac{\xi}{z},\Delta^2\right)\\
&= \frac{1}{2}\sum_{N,q} e_q \int_{-1}^{1} d\left(\frac{x}{z}\right) H_q^N\left(\frac{x}{z},\frac{\xi}{z},\Delta^2\right) \int_0^1 dz\, h_N^{^4\mathrm{He}}(z,\xi,\Delta^2)\\
&= \frac{1}{2}\sum_{N,q} F_q^N(\Delta^2) F_N^{^4\mathrm{He}}(\Delta^2) = F_C^{^4\mathrm{He}}(\Delta^2). \qquad (19)
\end{aligned}$$

In the above equation, F_q^N is the contribution of the quark q to the nucleon ff and $F_N^{^4\mathrm{He}}$ is the so called "point-like form factor", which would give the contribution of the nucleon N to the nuclear ff if the nucleons were point-like.

Let us note that the factor of 2 in the denominator of the above equation, i.e., the charge of the nucleus under scrutiny in units of e, guarantees the standard normalization $F_C^{^4\mathrm{He}}(0) = 1$. This quantity is shown in Fig. 4. Despite the approximated Δ dependence of the spectral function described in the previous section, reasonable agreement with the data [40] is obtained for the low values of $(-t)$ accessed by the EG6 experiment at JLab. The agreement has certainly to be improved evaluating a realistic spectral function of ^{4}He for a precise description of the accurate data of the next generation of measurements. The size of the target is reproduced with good accuracy. Quantitatively, we get $\sqrt{\langle r^2_{\mathrm{rms}}\rangle} \simeq 1.80$ fm to be compared with the experimental value of 1.671(14) fm [40]. In Fig. 4, for completeness, also the results for the nuclear form factor obtained within a one-body Av18 + UIX calculation, compared with data in Ref. [39], have been shown. Within a realistic Av18 + UIX spectral function, one would have obtained this kind of result for the nuclear ff. We stress anyway

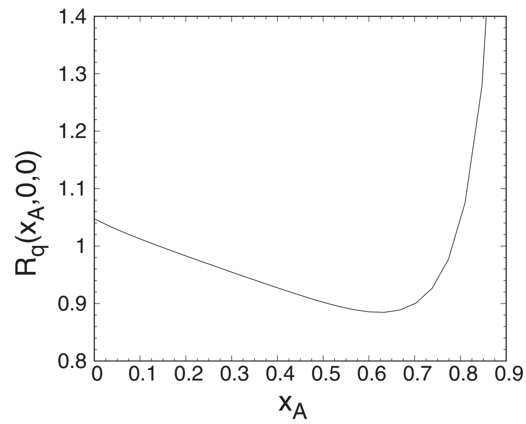

FIG. 5. The ratio Eq. (20) for the flavor $q = u$ (the result for $q = d$ is indistinguishable).

that the direct calculation of the ^{4}He ff requires only the wave function of the bound state, whereas the calculation through the GPDs, performed here as a check, requires all the wave functions of the spectral decomposition of ^{4}He.

As a second test, we checked that the obtained GPD has the expected forward limit. This is seen in Fig. 5, where the ratio,

$$R_q^{^4\mathrm{He}}(x_A) = H_q^{^4\mathrm{He}}(x_A,0,0)/H_q^N(x_A,0,0) \qquad (20)$$

is shown as a function of $x_A = M_A/Mx \simeq 4x$ to have an easy comparison with the results shown in the literature of DIS phenomena. In the above equation, the numerator is given by the forward limit of Eq. (10), and the denominator is given by the forward limit of the model used for the nucleon GPD. No relevant difference is found between the results for $q = u$ and $q = d$ as it is natural for an isoscalar nucleus. The typical EMC-like behavior found for this ratio in IA is reproduced. One should note anyway that the true EMC ratio is defined dividing the nucleus F_2 structure functions by the same quantity for the deuteron whereas the quantity shown here is obtained in terms of parton distributions of a given

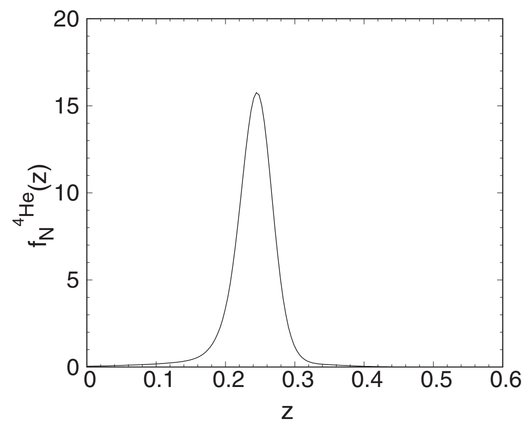

FIG. 6. The light-cone momentum distribution for the nucleon N in ^{4}He, Eq. (15).

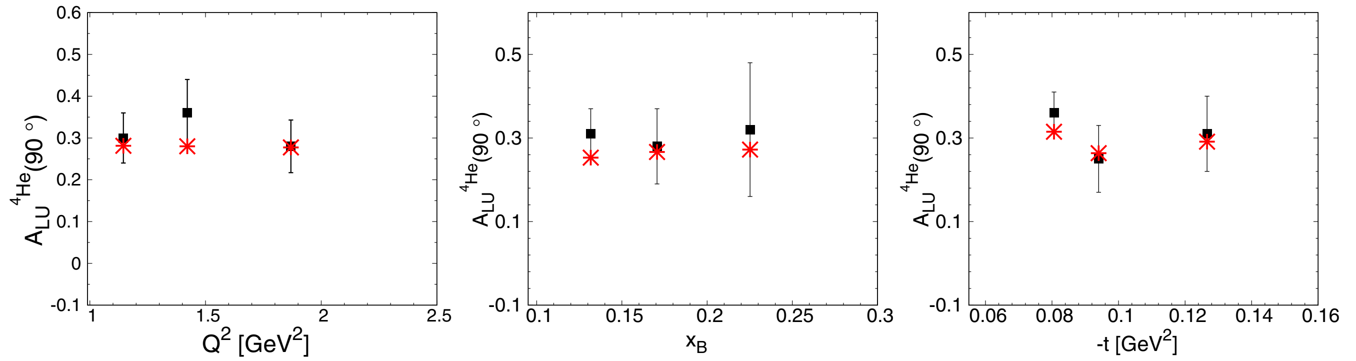

FIG. 7. ^{4}He azimuthal beam-spin asymmetry $A_{LU}(\phi)$ for $\phi = 90^\circ$: Results of this approach (red stars) compared with data (black squares) [30]. From left to right, the quantity is shown in the experimental Q^2, x_B, and t bins, respectively.

flavor. This behavior is therefore related to the EMC effect, but it represents a different quantity.

The results of checks (1) and (2) are therefore rather encouraging.

Size and relevance of nuclear effects can be inferred from the behavior of the light-cone momentum distribution Eqs. (11) and (15). If nuclear effects were negligible, these functions would be δ functions. The light-cone momentum distribution, in the forward limit, is shown in Fig. 6. One can see in passing that the present approach predicts a vanishing DVCS cross section already for ξ as small as 0.15, representing the width of the shown distribution. Indeed, ξ is the fraction of plus momentum transfer and cannot exceed the width of $f(z)$ if we want the target to be intact after the interaction. If, in future measurements, coherent DVCSs were observed at larger values of ξ, the role of non-nucleonic degrees of freedom would be exposed as suggested in the seminal paper [2].

Now, the comparison of our results with the data of the EG6 experiment is eventually performed.

In the EG6 experiment the crucial measured observable is the single-spin asymmetry A_{LU}, which can be extracted from the reaction yields for the two electron helicities ($N^{\pm}$),

$$A_{LU} = \frac{1}{P_B}\frac{N^+ - N^-}{N^+ + N^-}, \tag{21}$$

where P_B is the degree of longitudinal polarization of the incident electron beam. The DVCS amplitude depends on the GPDs. In EG6 kinematics, the cross section of real photon electroproduction is dominated by the Bethe-Heitler (BH) contribution, whereas the DVCS contribution is very small. However, the DVCS contribution is enhanced in the observables sensitive to the interference term, e.g., A_{LU}. The three terms entering the cross-sectional calculation, the squares of the BH and DVCS amplitudes, and their interference term, depend on the azimuthal angle ϕ between the (e,e') and the $(\gamma^*,{}^4\text{He}')$ planes as shown for the nucleon in Ref. [51] and for the spin-zero targets in Refs. [18,29]. Based on this paper, A_{LU} for a spin-zero hadron can be expressed at the leading twist as

$$A_{LU}(\phi) = \frac{\alpha_0(\phi)\text{Im}\,(\mathcal{H}_A)}{\alpha_1(\phi)+\alpha_2(\phi)\text{Re}\,(\mathcal{H}_A)+\alpha_3(\phi)[\text{Re}\,(\mathcal{H}_A)^2+\text{Im}\,(\mathcal{H}_A)^2]}. \tag{22}$$

Explicit forms for the kinematic factors α_i are derived from expressions in Ref. [29] and are functions of Fourier harmonics in the azimuthal angle ϕ, the nuclear form factor $F_A(t)$, and kinematical factors. Using the different $\sin(\phi)$ and $\cos(\phi)$ contributions, in the experimental analysis, both the imaginary and the real parts of the so-called Compton form factor $\mathcal{H}_A$ have

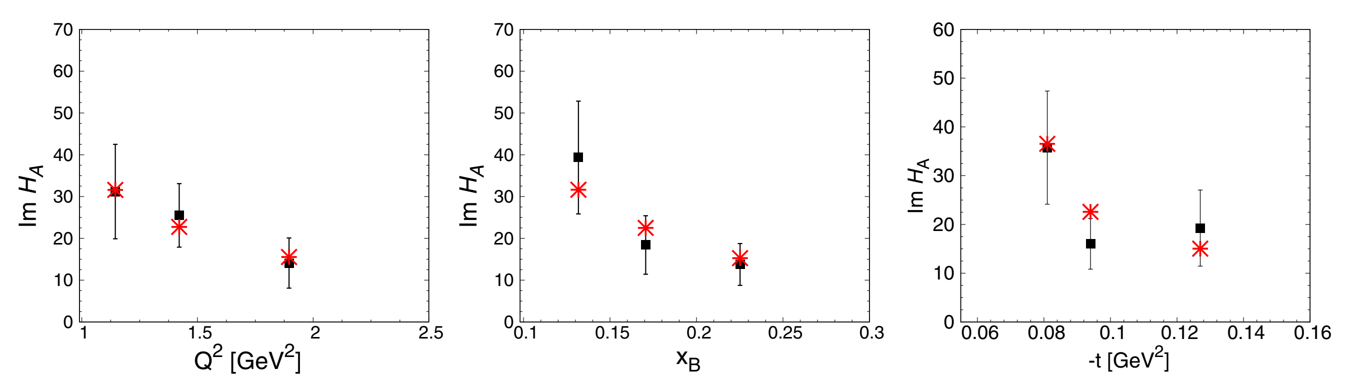

FIG. 8. The imaginary part of the Compton form factor for ^{4}He: Results of this approach (red stars) compared with data (black squares) [30]. From left to right, the quantity is shown in the experimental Q^2, x_B, and t bins, respectively.

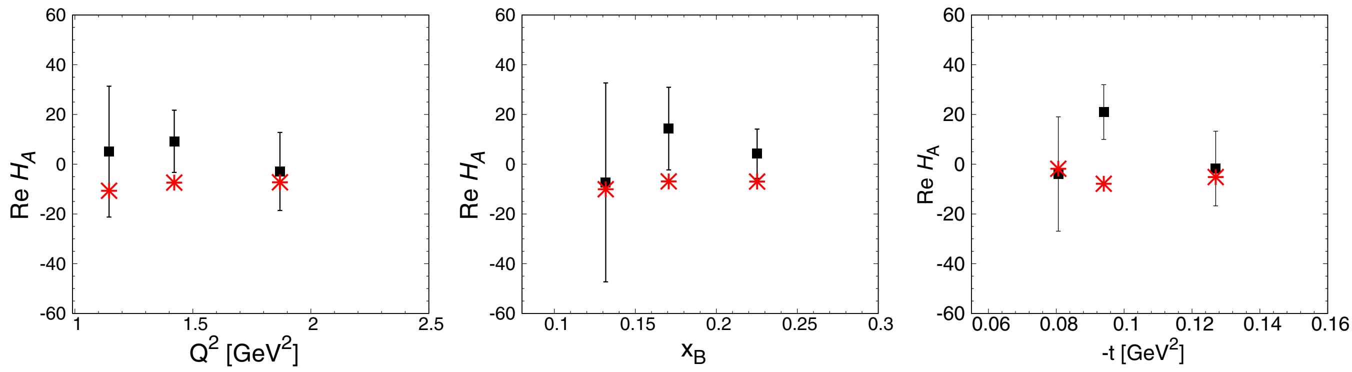

FIG. 9. The real part of the Compton form factor for ^{4}He: Results of this approach (red stars) compared with data (black squares) [30]. From left to right, the quantity is shown in the experimental Q^2, x_B, and t bins, respectively.

been extracted by fitting the $A_{LU}(\phi)$ distribution. In turn, the imaginary and real parts of $\mathcal{H}_A$ are defined as follows [52]:

$$\mathrm{Im}\,(\mathcal{H}_A) = H_A(\xi,\xi,t) - H_A(-\xi,\xi,t), \quad (23)$$

$$\mathrm{Re}\,(\mathcal{H}_A) = \mathrm{P}\int_0^1 dx[H_A(x,\xi,t) - H_A(-x,\xi,t)]\,C^+(x,\xi), \quad (24)$$

in terms of the nuclear GPD H_A, where P is the Cauchy principal-value integral and a coefficient function $C^+ = \frac{1}{x-\xi} + \frac{1}{x+\xi}$ has been introduced.

Using our result for the GPD of ^{4}He Eq. (10), we could evaluate Eqs. (22)–(24). Results are reported in Figs. 7–9, respectively, compared with the EG6 data.

In Fig. 7, A_{LU} is shown at $\phi = 90^\circ$ as a function of the kinematical variables Q^2, $x_B = Q^2/(2M\nu)$, and t. Due to limited statistics, in the experimental analysis these latter variables have been studied separately with a two-dimensional data binning. The same procedure has been used in our theoretical estimate. For example, each point at a given x_B has been obtained using for t and Q^2 the corresponding average experimental values. Overall, very good agreement is found.

The same happens for $\mathrm{Im}\,(\mathcal{H}_A)$ shown in Fig. 8, whereas for $\mathrm{Re}\,(\mathcal{H}_A)$ the agreement is somehow less satisfactory as is seen in Fig. 9. In particular, one point in the t dependence is not reproduced. One should not forget anyway that the present data do not constrain enough $\mathrm{Re}\,(\mathcal{H}_A)$, a quantity appearing multiplied by small coefficients in Eq. (22).

The Cauchy principal-value integral in Eq. (24) has been evaluated numerically using both the standard Cern library routines and the procedure described in Ref. [53] obtaining a negligible difference with the two methods. From the theoretical side we note also that the result for $\mathrm{Re}\,(\mathcal{H}_A)$ is strongly dependent on the model used to evaluate the nucleon GPD in the convolution formula. We also note that the GK model is supposed to work properly at $Q^2 > 4$ GeV^2. Here we have forced its validity at much lower-Q^2 values with remarkable success.

In the light of this comparison, we can conclude that the description of the present data does not require exotic arguments, such as dynamical off shellness. As a matter of fact, our calculation shows that careful use of basic conventional ingredients is able to reproduce the data.

V. CONCLUSIONS AND PERSPECTIVES

A thorough analysis of the available data on coherent deeply virtual Compton scattering off ^{4}He has been presented. The framework is the impulse approximation description of the process at leading twist, given by the handbag contribution. In this way, a convolution formula is obtained, in terms of a nondiagonal one-body spectral function of the nucleus and the GPD of the bound nucleon. The nucleonic contribution is parametrized through the Goloskokov-Kroll model. The nuclear part is given by a model of the one-body nondiagonal spectral function, which reproduces in the proper limit the exact Av18 + UIX diagonal momentum distribution. A reasonable description of the electromagnetic form factor at the low values of the momentum transfer, relevant for the specific experimental kinematics, is reproduced. In the forward limit, the nuclear parton distributions show the expected EMC-like behavior. Overall very good agreement is found for the observables recently measured at Jefferson Laboratory. As a matter of fact, our calculation shows that a careful analysis of the reaction mechanism in terms of basic conventional ingredients is able to describe the data. We can conclude that the present experimental accuracy does not require the use of exotic arguments, such as dynamical off shellness. Nevertheless, a serious benchmark calculation in the kinematics of the next generation of precise measurements at high luminosity will require an improved treatment of both the nucleonic and the nuclear parts of the calculation. The latter task includes the realistic evaluation of a one-body nondiagonal spectral function of ^{4}He. Work is in progress towards this challenging direction. In the meantime, the straightforward approach proposed here can be used as a workable framework for the planning of future measurements.

ACKNOWLEDGMENTS

We warmly thank R. Dupré and M. Hattaway for many helpful explanations on the EG6 experiment and L. E. Marcucci for sending us the results for the one-body form factor calculation within the AV18 + UIX potential, shown in Ref. [39] and reproduced here in Fig. 4.

[1] R. Dupré and S. Scopetta, Eur. Phys. J. A **52**, 159 (2016).
[2] E. R. Berger, F. Cano, M. Diehl, and B. Pire, Phys. Rev. Lett. **87**, 142302 (2001).
[3] J. J. Aubert *et al.* (European Muon Collaboration), Phys. Lett. B **123**, 275 (1983).
[4] O. Hen, D. W. Higinbotham, G. A. Miller, E. Piasetzky, and L. B. Weinstein, Int. J. Mod. Phys. E **22**, 1330017 (2013).
[5] A. Airapetian *et al.* (HERMES Collaboration), Phys. Rev. C **81**, 035202 (2010).
[6] M. V. Polyakov, Phys. Lett. B **555**, 57 (2003).
[7] H. C. Kim, P. Schweitzer, and U. Yakhshiev, Phys. Lett. B **718**, 625 (2012).
[8] J. H. Jung, U. Yakhshiev, H. C. Kim, and P. Schweitzer, Phys. Rev. D **89**, 114021 (2014).
[9] A. Freund and M. Strikman, Eur. Phys. J. C **33**, 53 (2004).
[10] A. Freund and M. Strikman, Phys. Rev. C **69**, 015203 (2004).
[11] S. Liuti and S. K. Taneja, Phys. Rev. D **70**, 074019 (2004).
[12] V. Guzey and M. Siddikov, J. Phys. G: Nucl. Part. Phys. **32**, 251 (2006).
[13] S. Liuti and S. K. Taneja, Phys. Rev. C **72**, 034902 (2005).
[14] K. Goeke, V. Guzey, and M. Siddikov, Phys. Rev. C **79**, 035210 (2009).
[15] V. Guzey, Phys. Rev. C **78**, 025211 (2008).
[16] V. Guzey, A. W. Thomas, and K. Tsushima, Phys. Lett. B **673**, 9 (2009).
[17] V. Guzey, A. W. Thomas, and K. Tsushima, Phys. Rev. C **79**, 055205 (2009).
[18] A. Kirchner and D. Mueller, Eur. Phys. J. C **32**, 347 (2003).
[19] F. Cano and B. Pire, Eur. Phys. J. A **19**, 423 (2004).
[20] S. K. Taneja, K. Kathuria, S. Liuti, and G. R. Goldstein, Phys. Rev. D **86**, 036008 (2012).
[21] R. B. Wiringa, V. G. J. Stoks, and R. Schiavilla, Phys. Rev. C **51**, 38 (1995).
[22] S. Scopetta, Phys. Rev. C **70**, 015205 (2004).
[23] S. Scopetta, Phys. Rev. C **79**, 025207 (2009).
[24] M. Rinaldi and S. Scopetta, Phys. Rev. C **85**, 062201 (2012).
[25] M. Rinaldi and S. Scopetta, Phys. Rev. C **87**, 035208 (2013).
[26] M. Rinaldi and S. Scopetta, Few Body Syst. **55**, 861 (2014).
[27] V. Guzey and M. Strikman, Phys. Rev. C **68**, 015204 (2003).
[28] S. Liuti and S. K. Taneja, Phys. Rev. C **72**, 032201 (2005).
[29] A. V. Belitsky and D. Müller, Phys. Rev. D **79**, 014017 (2009).
[30] M. Hattawy *et al.* (CLAS Collaboration), Phys. Rev. Lett. **119**, 202004 (2017).
[31] W. R. Armstrong *et al.* (ALERT Collaboration), arXiv:1708.00888.
[32] W. R. Armstrong *et al.* (ALERT Collaboration), arXiv:1708.00835.
[33] J. C. Collins, L. Frankfurt, and M. Strikman, Phys. Rev. D **56**, 2982 (1997).
[34] M. Diehl, Phys. Rep. **388**, 41 (2003).
[35] C. Ciofi degli Atti and S. Liuti, Phys. Rev. C **41**, 1100 (1990).
[36] A. Del Dotto, E. Pace, G. Salmè, and S. Scopetta, Phys. Rev. C **95**, 014001 (2017).
[37] H. Morita and T. Suzuki, Prog. Theor. Phys. **86**, 671 (1991).
[38] V. D. Efros, W. Leidemann, and G. Orlandini, Phys. Rev. C **58**, 582 (1998).
[39] A. Camsonne *et al.* (Jefferson Lab Hall A Collaboration), Phys. Rev. Lett. **112**, 132503 (2014).
[40] C. R. Ottermann, G. Kobschall, K. Maurer, K. Rohrich, C. Schmitt, and V. H. Walther, Nucl. Phys. **A436**, 688 (1985).
[41] M. Viviani, A. Kievsky, and S. Rosati, Phys. Rev. C **71**, 024006 (2005).
[42] A. Kievsky, S. Rosati, and M. Viviani, Nucl. Phys. **A551**, 241 (1993).
[43] A. Kievsky, S. Rosati, M. Viviani, L. E. Marcucci, and L. Girlanda, J. Phys. G: Nucl. Part. Phys. **35**, 063101 (2008).
[44] B. S. Pudliner, V. R. Pandharipande, J. Carlson, and R. B. Wiringa, Phys. Rev. Lett. **74**, 4396 (1995).
[45] M. Viviani, A. Kievsky, and A. S. Rinat, Phys. Rev. C **67**, 034003 (2003).
[46] A. S. Rinat, M. F. Taragin, and M. Viviani, Phys. Rev. C **72**, 015211 (2005).
[47] C. Ciofi degli Atti and S. Simula, Phys. Rev. C **53**, 1689 (1996).
[48] S. V. Goloskokov and P. Kroll, Eur. Phys. J. C **53**, 367 (2008).
[49] S. V. Goloskokov and P. Kroll, Eur. Phys. J. A **47**, 112 (2011).
[50] A. V. Radyushkin, Phys. Rev. D **59**, 014030 (1998).
[51] A. V. Belitsky, D. Mueller, and A. Kirchner, Nucl. Phys. **B629**, 323 (2002).
[52] M. Guidal, H. Moutarde, and M. Vanderhaeghen, Rep. Prog. Phys. **76**, 066202 (2013).
[53] B. Bialecki and P. Keast, J. Comput. Appl. Math. **112**, 3 (1999).